

# STM spectroscopy on superconducting $\text{FeSe}_{1-x}\text{Te}_x$ single crystals at 300 mK

I. Fridman<sup>a</sup>, K.-W. Yeh<sup>b</sup>, M.-K. Wu<sup>b</sup>, J.Y.T. Wei<sup>a,c,\*</sup>

<sup>a</sup> Department of Physics, University of Toronto, ON, Canada M5S1A7

<sup>b</sup> Institute of Physics, Academia Sinica, Taipei, Taiwan

<sup>c</sup> Canadian Institute for Advanced Research, Toronto, ON, Canada M5G1Z8

## ARTICLE INFO

Available online 7 October 2010

Keywords:

C. Scanning tunnelling microscopy (STM)

D. Superconductivity

## ABSTRACT

We report cryogenic scanning tunneling spectroscopy measurements on single crystals of superconducting  $\text{FeSe}_{1-x}\text{Te}_x$ , at doping levels of  $x=0.5$  and  $0.7$ , with critical temperatures  $T_c \approx 12$  K. Atomically resolved topographic images were obtained, showing large-scale density-of-state clustering which appears to have no periodicity and to vary with the doping. Conductance spectra taken at 300 mK showed a generally asymmetric V-shaped background, along with a sharp dip structure within  $\sim \pm 2-4$  mV. These spectra appeared to vary over  $\sim$  nm length scale, and not correlated with the topography. The overall spectral evolution versus temperature is consistent with the dip structure arising from a superconducting energy gap which closes above  $T_c$ , and with the spectral background having a non-superconducting origin. The persistence of finite zero-bias conductance down to 300 mK, well below  $T_c$ , indicates the presence of low-energy quasiparticles on parts of the Fermi surface. We discuss our data in light of some other recent spectroscopic measurements of  $\text{FeSe}_{1-x}\text{Te}_x$ , and in terms of its characteristic band structure.

© 2010 Elsevier Ltd. All rights reserved.

## 1. Introduction

$\text{FeSe}_{1-x}\text{Te}_x$  is a recently discovered iron-based superconductor with a superconducting critical temperature ( $T_c$ ) ranging from 8 to 14 K [1,2]. This so-called “11” system is comprised of Fe atoms on a square lattice surrounded by chalcogen tetrahedra, a structure similar to the planar Fe–As sublattice in the Fe-pnictides. Doping of the chalcogen sites appears to drive the  $\text{FeSe}_{1-x}\text{Te}_x$  system between superconductivity and magnetism. While FeTe is known to be an antiferromagnetic metal [3], the occurrence of superconductivity in the non-magnetic FeSe has been related to spin fluctuations [4]. A host of bulk and microscopic probes have indicated the coexistence of incommensurate magnetism and superconductivity as a function of the doping [5], as well as possible phase segregation giving rise to non-bulk superconductivity within a finite doping regime [6]. There has also been evidence for spatial variations in the Fe content [7], with excess Fe possibly playing a local role in the interplay between the magnetism and superconductivity.

## 2. Experimental details

Scanning tunneling microscope (STM) is a powerful local probe that is used to acquire surface topographic images as well as conductance spectra related to the quasiparticle density-of-states

(DOS). The home-built cryomagnetic STM used in this experiment was specially designed to operate down to 300 mK and up to 9 T. The Pt–Ir tips used were cleaned in-situ with field emission to ensure their robustness. RF-filters were used throughout the STM wiring to achieve maximum energy resolution down to base temperature. The tunneling conductance  $dI/dV$  data were acquired using lock-in amplification, with the sample biased relative to the tip. Single crystals of  $\text{FeSe}_{1-x}\text{Te}_x$ , with nominal Te compositions of  $x=0.5$  and  $0.7$ , were grown using the optical zone-melting technique [8]. X-ray diffraction indicated single-phase samples having the Pb–O structure, while magnetic and resistivity measurements showed robust superconducting transitions with onset temperatures of 13.1 and 13.6 K and transition widths of 2.2 and 1.5 K for the  $x=0.5$  and  $0.7$  samples, respectively. The as-grown crystals were sealed in dry ampules during transport, and then mounted into the STM and cleaved in vacuum to expose fresh surfaces just prior to cool down.

## 3. Results and discussion

Fig. 1 shows a typical STM topographic image taken on an  $x=0.5$  crystal at 4.2 K. The topograph was taken at 1 nA tunneling current with 10 mV bias, and reveals an atomic lattice with the expected periodicity of  $3.8 \text{ \AA}$  for a (0 0 1) chalcogenide surface. Also noticeable are larger clusters of DOS modulations over  $\sim$  nm length scale. Fourier transform of the topographic data did not reveal any periodicity for this clustering, indicating that it has no long range order at least within the STM scan range of

\* Corresponding author at: Department of Physics, University of Toronto, ON, Canada M5S1A7.

E-mail address: [wei@physics.utoronto.ca](mailto:wei@physics.utoronto.ca) (J.Y.T. Wei).

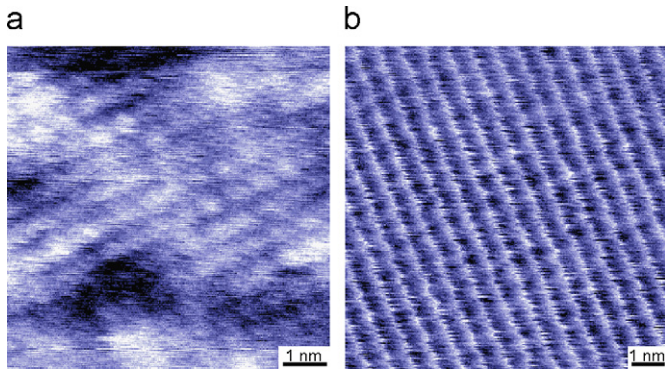


**Fig. 1.** STM topography taken on an  $\text{FeSe}_{0.5}\text{Te}_{0.5}$  samples at 4.2 K. An atomically resolved surface with periodicity of 3.8 Å is seen in the 25 nm image (a) and detail (b), corresponding to a (001) chalcogenide surface. Clusters of bright and dark regions  $\sim$  several nm in size are also observed, with no apparent periodicity over larger length scales.

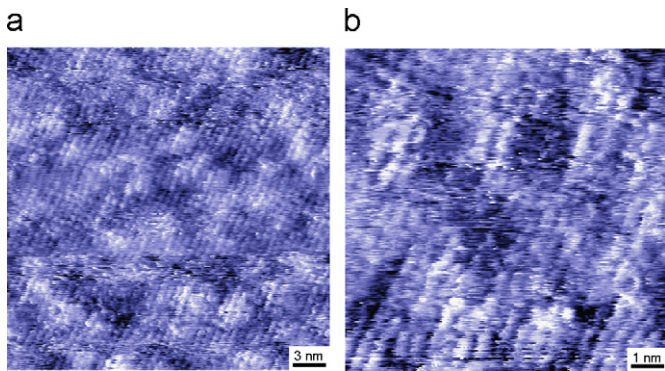


**Fig. 2.** STM topographic image taken on an  $\text{FeSe}_{0.3}\text{Te}_{0.7}$  sample at 300 mK. Topography is predominantly composed of regions with clusters, as shown in (a), similar to what is observed on the  $x=0.5$  sample, but homogeneous regions are sometimes seen, as shown in (b).

$\sim 500 \text{ nm} \times 500 \text{ nm}$ . Atomically resolved topographs taken on  $x=0.7$  crystals also showed large-scale DOS clustering, as displayed in Fig. 2, although homogeneous regions  $\sim 100 \text{ nm} \times 100 \text{ nm}$  in area were also observed. This difference indicates that the doping could be systematically affecting the DOS clustering, although it is not yet clear whether the clustering is due to either chemical or electronic inhomogeneity. Here we note that similar DOS clustering has also been observed on  $x=0.55$  crystals by both STM and low-energy electron diffraction [7,9], and could be attributed to either local oxidation, vacancies at Se/Te sites, or excess Fe at interstitial sites. To determine the detailed chemical composition of the DOS clusters observed on our samples, we will carry out refined local structural analysis using both X-ray and neutron scattering [11].

Fig. 3 shows the STM spectroscopy data taken at various positions on an  $x=0.7$  crystal at 300 mK. The  $dI/dV$  spectra generally have asymmetric V-shaped backgrounds that dip sharply at low voltages, indicating the presence of an energy gap  $\sim 4 \text{ meV}$  to  $\sim 8 \text{ meV}$  in size from one gap edge to the other. Also noticeable are small “sugbap” inflections within the dip structure, ranging between  $\sim \pm 1$  and  $\sim \pm 2 \text{ mV}$  in position. Despite the clear sharp dip,  $dI/dV$  does not reach zero at zero bias voltage, indicating finite DOS at the Fermi level. These observations are in generic agreement with the STM spectroscopy data of Ref. [9], as well as with the angle-resolved photoemission spectroscopy (ARPES) data of Ref. [10], although both of the latter data were taken at higher temperatures. It is worth noting that the gap-like structures and the spectral background in our

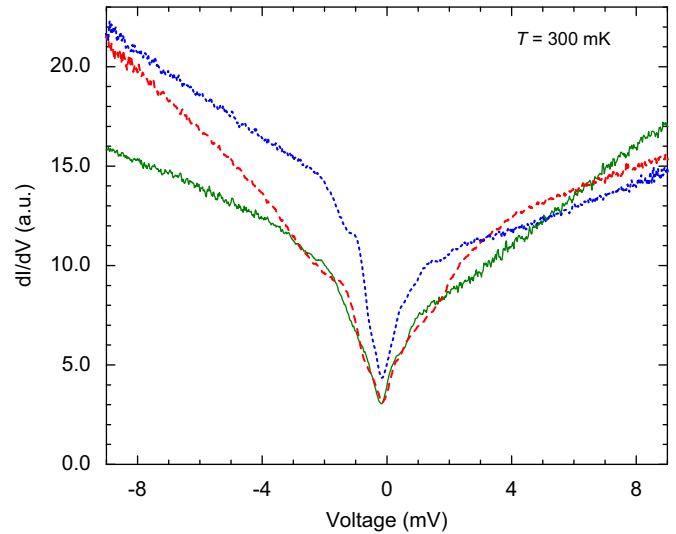


**Fig. 3.** STM conductance spectra taken at various positions on an  $\text{FeSe}_{0.3}\text{Te}_{0.7}$  samples at 300 mK. The spectra have an asymmetric V-shaped background that develops into a sharp dip at low energies, indicating the presence of an energy gap  $\sim 4$  to  $\sim 8 \text{ meV}$  in size from one gap edge to the other. Both the background conductance and the dip structure showed spatial variation over  $\sim \text{nm}$  length scale.

measurements showed spatial variation over  $\sim \text{nm}$  length scale, suggesting that these spectral features may be related to the DOS clustering described above. To further examine this possibility, we will carry out more detailed STM measurements to look for clear correlations between the topography and spectroscopy.

Fig. 4 shows the typical temperature dependence of the STM spectroscopy data taken on an  $x=0.7$  crystal. The spectra are staggered vertically for clarity, and normalized by dividing each curve by the conductance at 10 mV bias. As temperature is increased from 300 mK to 4.2 K, the sharp spectral dip becomes a rounded depression with a gap-like inflection for only positive bias, while the asymmetric background is largely preserved. Furthermore, as the temperature is raised to 13 K, above  $T_c$ , the gap-like structure vanishes across the spectrum, leaving only a parabolic profile which is relatively symmetric. Despite the persistence of a non-uniform spectral background, the zero-bias  $dI/dV$  clearly rises with increasing temperature, consistent with the closing of an energy gap. Here again we note that there was considerable spectral variation over  $\sim \text{nm}$  length scale, in both the spectral asymmetry and gap-like structures we observed. More detailed measurements and spectral analysis are needed to quantitatively relate the observed spectral evolution with temperature dependence of the superconducting energy gap.

To understand the origin of the spectral background, we consider effects of the band structure on the quasiparticle DOS spectrum. First, V-shaped spectral backgrounds have been previously observed in quasiparticle tunneling on cuprate superconductors, and attributed to their characteristic band structures [12]. For  $\text{FeSe}_{1-x}\text{Te}_x$ , just as for the Fe-pnictides, it is believed that the Fermi level crosses both electron and hole bands [15]. This ostensibly multiband feature of  $\text{FeSe}_{1-x}\text{Te}_x$  could provide a natural source of electron–hole asymmetry which is manifested as spectral asymmetry in the quasiparticle DOS at sufficiently high energies. It should be remarked that other mechanisms of spectral asymmetry have also been proposed, for example in relation to the predominance of hole superconductivity [13] or to the interplay of superconductivity with coexisting order parameters [14].

To explain the non-vanishing DOS at the Fermi level, we also consider the Fermi surface (FS) topology of  $\text{FeSe}_{1-x}\text{Te}_x$ . First,

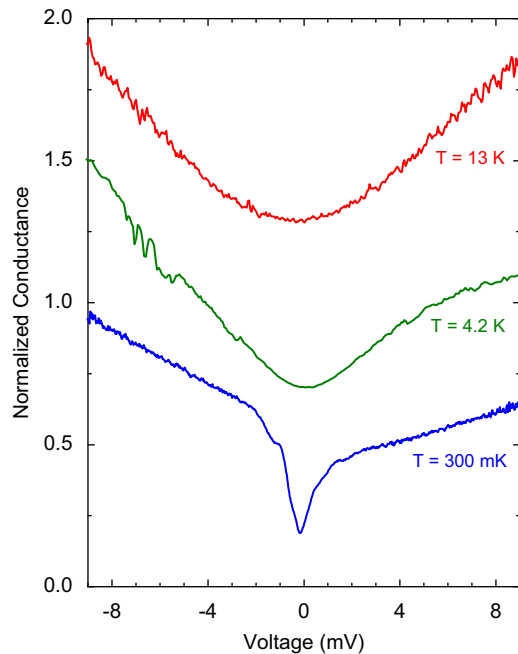


**Fig. 4.** Temperature dependence of the STM spectroscopy data taken on an  $\text{FeSe}_{0.3}\text{Te}_{0.7}$  samples, with  $T_c \approx 12$  K. Spectra are shifted vertically and normalized (see text). The parabolic background above  $T_c$  develops a depression at low energy with decreasing temperature, and develops a sharp dip at the lowest temperature.

band-structure calculations that take excess Fe into account have indicated three FS sheets at the  $\Gamma$  point [15], in contrast to the Fe-pnictides which are believed to have only two such sheets [16]. It has been suggested that the extra FS pocket may be uncondensed below  $T_c$ , thereby introducing finite DOS near zero quasiparticle energy, even at 300 mK which is well below  $T_c$ . Because of the smallness of this FS pocket, minor variations in the doping could shift it away from the Fermi level, thus explaining variations in the gap-like structures observed [17,18]. Further work is needed to elucidate this issue, by comparing details of the calculated and measured band structure, using both ARPES and STM spectroscopy.

#### 4. Conclusion

In summary, cryogenic scanning tunneling spectroscopy was performed on single crystals of superconducting  $\text{FeSe}_{1-x}\text{Te}_x$ , at doping levels of  $x=0.5$  and  $0.7$ . Atomically resolved topographic images were obtained, showing large-scale density-of-state clustering which appears to vary with sample doping and to have no periodicity on the surface. Conductance spectra taken at 300 mK vary over  $\sim$  nm length scale and did not appear to correlate with the topography. Spectra showed a generally asymmetric V-shaped background, along with a sharp dip within  $\sim \pm 2-4$  mV. The persistence of finite zero-bias conductance at

the lowest temperature indicates the presence of low-energy quasiparticles on parts of the Fermi surface. The overall spectral evolution versus temperature is consistent with the dip structure arising from a superconducting energy gap which opens below  $T_c$ , and with the spectral background having a non-superconducting origin. Our observations are in generic agreement with other recent STS and ARPES measurements on  $\text{FeSe}_{1-x}\text{Te}_x$ , and could be qualitatively explained in terms of the characteristic band structure of this compound. Further work correlating real-space and reciprocal-space measurements is needed to elucidate the origin of the topographic and spectroscopic inhomogeneities observed, particularly in terms of chemical and structural variations.

#### Acknowledgments

The research work in Toronto was supported by NSERC, CFI, OIT, and the Canadian Institute for Advanced Research under the Quantum Materials Program. The research work in Taiwan was supported by the National Science Council.

#### References

- [1] F.-C. Hsu, J.-Y. Luo, K.-W. Yeh, T.-K. Chen, T.-W. Huang, P.M. Wu, Y.-C. Lee, Y.-L. Huang, Y.-Y. Chu, D.-C. Yan, M.-K. Wu, Proc. Natl. Acad. Sci. 105 (2008) 14262.
- [2] K.-W. Yeh, T.-W. Huang, Y.-L. Huang, T.-K. Chen, F.-C. Hsu, P.M. Wu, Y.-C. Lee, Y.-Y. Chu, C.-L. Chen, J.-Y. Luo, D.-C. Yan, M.-K. Wu, Eur. Phys. Lett. 84 (2008) 37002.
- [3] S. Li, C. de la Cruz, Q. Huang, Y. Chen, J.W. Lynn, J. Hu, Y.-L. Huang, F.-C. Hsu, K.-W. Yeh, M.-K. Wu, P. Dai, Phys. Rev. B 79 (2009) 054503.
- [4] T. Imai, K. Ahilan, F.L. Ning, T.M. McQueen, R.J. Cava, Phys. Rev. Lett. 102 (2009) 177005.
- [5] R. Khasanov, M. Bendele, A. Amato, P. Babkevich, A.T. Boothroyd, A. Cervellino, K. Conder, S.N. Gvasaliya, H. Keller, H.-H. Klauss, H. Luetkens, V. Pomjakushin, E. Pomjakushina, B. Roessli, Phys. Rev. B 80 (2009) 140511.
- [6] T.J. Liu, J. Hu, B. Qian, D. Fobes, Z.Q. Mao, W. Bao, M. Reehuis, S.A.J. Kimber, K. Prokes, S. Matas, D.N. Argyriou, A. Hiess, A. Rotaru, H. Pham, L. Spinu, Y. Qiu, V. Thampy, A.T. Savici, J.A. Rodriguez, C. Broholm, arXiv:1003.5647v1.
- [7] F. Massee, S. de Jong, Y. Huang, J. Kaas, E. van Heumen, J.B. Goedkoop, M.S. Golden, Phys. Rev. B 80 (2009) 140507.
- [8] K.W. Yeh, C.T. Ke, T.W. Huang, T.K. Chen, Y.L. Huang, P.M. Wu, M.K. Wu, Crystal Growth Des. 9 (2009) 4847.
- [9] T. Kato, Y. Mizuguchi, H. Nakamura, T. Machida, H. Sakata, Y. Takano, Phys. Rev. B 80 (2009) 180507.
- [10] K. Nakayama, T. Sato, P. Richard, T. Kawahara, Y. Sekiba, T. Qian, G.F. Chen, J.L. Luo, N.L. Wang, H. Ding, T. Takahashi, arXiv:0907.0763v1.
- [11] R. Hu, E.S. Bozin, J.B. Warren, C. Petrovic, Phys. Rev. B 80 (2009) 214514.
- [12] J.Y.T. Wei, C.C. Tsuei, P.J.M. van Bentum, Q. Xiong, C.W. Chu, M.K. Wu, Phys. Rev. B 57 (1998) 3650.
- [13] J.E. Hirsch, Phys. Rev. B 59 (1999) 11962.
- [14] J.-P. Hu, K. Seo, Phys. Rev. B 73 (2006) 094523.
- [15] F. Chen, B. Zhou, Y. Zhang, J. Wei, H.-W. Ou, J.-F. Zhao, C. He, Q.-Q. Ge, M. Arita, K. Shimada, H. Namatame, M. Taniguchi, Z.-Y. Lu, J. Hu, X.-Y. Cui, D.L. Feng, Phys. Rev. B 81 (2010) 014526.
- [16] C. Liu, G.D. Samolyuk, Y. Lee, N. Ni, T. Kondo, A.F. Santander-Syro, S.L. Bud'ko, J.L. McChesney, E. Rotenberg, T. Valla, A.V. Fedorov, P.C. Canfield, B.N. Harmon, A. Kaminski, Phys. Rev. Lett. 101 (2008) 177005.
- [17] For example, see recent STS data for  $x=0.45$  by T. Hanaguri, S. Niitaka, K. Kuroki, H. Takagi, Science 328 (2010) 474.
- [18] B. Zeng, G. Mu, H.Q. Luo, T. Xiang, H. Yang, L. Shan, C. Ren, I.I. Mazin, P.C. Dai, H.-H. Wen, arXiv:1007.3597v1 [cond-mat.supr-con].